A TEST FOR INTERFACIAL EFFECTS AND STRESS TRANSFER IN CERAMIC MATRIX COMPOSITES

NASA GRANT NAG 2-444
PROGRESS REPORT
For The Period Sept.1, 1987 To April 1, 1988

Prepared For
AMES Research Center
National Aeronautics and Space Administration
Moffet Field, CA 94035

From
Department of Materials Science and Engineering
University of Utah
Salt Lake City, Utah, 84112

ABSTRACT

A test specimen has been devised for measuring stress transfer between a high modulus fiber and a ceramic matrix. Single filaments of SiC were embedded in chemically vapor deposited SiC on a thin plate of molybdenum. The CVD overcoating which encapsulated the fiber was continuous with a coating of SiC on the molybdenum. When placed in a microtensile test device and loaded in the fiber direction, the fiber fracture characteristics provide information on the fiber/matrix adhesion and stress transfer.

Problems were encountered due to the formation of a weak boundary between the SiC and the molybdenum with obviated any meaningful tensile tests. Also, the high CVD temperature used in fabricating these specimens restricts the fiber, matrix (and substrate) to materials having similar thermal coefficients of expansion in order to minimize thermal stresses.

1. INTRODUCTION

Fiber reinforced ceramic matrix composites have recently received a great deal of attention[1-3] for possible application in engines, as thermal protection materials, and for special electronic/electrical devices. The primary reason for the interest in these materials is the expectation that strong ceramic fibers can prevent catastrophic brittle failure in ceramics by providing various energy dissipation processes during crack propagation. Early work utilizing carbon fibers in ceramic matrices demonstrated the potential for this approach[4,5]. However, carbon fibers are vulnerable to degradation in oxidizing reaction environments at relatively low temperatures; much below the use temperature of the ceramic materials. However, silicon carbide fibers (SiC) are more oxidation resistant than carbon fibers and are chemically compatible with many ceramic matrices.

Fiber-reinforcement of ceramics should, in principle, increase the resistance of the ceramic matrix. In general, this improved toughness has not been fully realized. Figure 1 represents the load sharing for strong bonding (A) and weak bonding (B). If as in Figure 1A, the redistribution length is short then the overload is highly concentrated so that a single fiber break could initiate breaks in adjacent fibers and possibly catastrophic failure of the composite. On the other hand, if the shear stress at a fiber break is large enough to cause debonding some distance from the fiber end then load is distributed over a longer fiber length and is less likely to fracture adjacent fibers (Figure 1B). Clearly, there must be some optimum boundary strength. If the interfacial strength is too low there will be excessive debonding and a loss in the load bearing capability of the fibers. However, a fundamental lack of information on how the

fiber/matrix interphases effects the overall failure of ceramic composites under an applied stress condition still exists. The factors which will influence the properties of a fiber matrix interphase are 1) the mechanical properties of the components themselves and 2) the degree of physical and chemical interaction between the fiber and matrix. Compared with the conventional ceramics, where the tensile strength is used for predicting engineering performance, the mechanical behavior of ceramic composites is much more complicated. The interphase properties are one of the major complications so there is a need to develop techniques to study fiber/matrix interphases, especially, the degree of adhesion.

Bascom et. al.[6] have successfully used a microscale (25 mm gauge length) "dogbone" specimens with single carbon fiber embedded through the length of the specimen as a method for determining the fiber/resin interphase strength for polymer matrix composites. A schematic of the single fiber test specimen in organic matrix system is shown in Figure 2. The work reported here originated from the idea that this technique could be applied to the fiber/ceramic matrix systems.

The purpose of this research during the last five months was to demonstrate the feasibility of developing a test method for the properties of the interphases between single embedded SiC fiber and silicon carbide matrix grown by chemical vapor deposition (CVD).

II. EXPERIMENTAL PROCEDURE

Silicon carbide coatings were applied to three different pure metal substrates; Ni*, W**, and Mo** with 99.995% purity. Table 1 summarizes the various properties of each metal substrate. The substrates were cut (1.5 cm X 3.5 cm X 0.2 cm) by using a low speed diamond saw and polished on sand paper. For information on the influence of substrate surface, the molybdenum plates were ground, polished and ion milled to 3000Å thickness by using an argon source to remove any contamination and heavy oxide layers.

An initial silicon carbide coating was deposited using a hot-wall horizontal silica tube reactor. Figure 3 shows a schematic diagram of laboratory reactor for the deposition of coatings on planar substrates. Dimethyldichlorosilane (DMDCS)*** was used as both the silicon and carbon sources. The DMDCS was injected into a manifold by bubbling through with argon gas, and was mixed with and carried by hydrogen into the reaction chamber. The total flow rate was kept constant between 0.2-0.3 mole/hour, and the pressure of the reactor was maintained at 1atm throughout this study.

The substrates were preheated at the deposition temperature and maintained in a flow of hydrogen for a minimum of 10 minutes prior to each deposition run. The substrate temperatures ranged from 1040 to 1060°C measured by means of a thermocouple at the substrate. One of the problems of the horizontal reactor is the depletion of the reactant in the downstream direction which results in thinner downstream deposits[7]. This was corrected by slightly tilting the substrates, thus diminishing the reactor cross section in the downstream direction. When the first layer of silicon carbide coating (~20μm) was applied, the sample was slowly drawn from the reactor to ambient temperature using a silica rod. This

procedure was used for all of the silicon carbide depositions.

Two different fibers (carbon and Nicalon SiC) were obtained from Hercules[+] and NASA[++], respectively and their typical properties are summarized in Table II and III. A single fiber was positioned lengthwise on top of the first layer of silicon carbide (undercoating) by using a high temperature paste (Sauereisen). The fiber was overcoated by growing another silicon carbide layer using the same conditions as for the first layer. The thickness of the deposited silicon carbide layer was determined by comparing the diameter of uncoated Nicalon SiC fiber with the deposited layer.

The crystalline phases present in silicon carbide depositions were identified by X-ray diffraction using Cu $K\alpha$ radiation.

III. RESULTS and DISCUSSION

The study of the formation of a brittle zone at the fiber/matrix interphase and of its influence on mechanical properties of ceramic fiber inorganic matrix composites should certainly be a major aspect of research, especially when it is necessary to choose appropriate intermediate layers between the fibers and the matrix.

Preliminary tests showed that the nature of the substrate had little influence upon the structure of the deposit but it had strong influence upon the thermal expansion coefficient mismatch ($\Delta\alpha$) between the substrate and coating. Initially, nickel plate was used as a substrate. The undercoating turned out to be uniform throughout the substrate. Optical micrographs of a silicon carbide undercoating on nickel substrate are shown in Figure 4. The deposits are fairly smooth and the surface of substrate was completely covered with a film having an approximately equal ratio of pentagon and hexagon grains. The overcoating of the carbon fiber, however, showed a number of cracks and peeled off the substrate. This implies that the adhesion becomes very poor as the thickness of coating increases. Figure 5 shows the optical micrograph of cracks and peeling of the coating and resulting damage on the fiber. The primary reason for the peeling of the coating is the thermal expansion coefficient mismatch ($\Delta\alpha = 10.2 \times 10^{-6}/^{o}k$) between the nickel substrate and the grown silicon carbide coating. Furthermore, the carbon fiber positioned lengthwise showed a number of breakages due to a large thermal expansion coefficient mismatch between the nickel substrate and carbon fiber and probably due to chemical attack of the gas phase components used in the CVD process. As mentioned earlier, SiC fiber is more stable at high temperature and in the CVD gas phase. Therefore, Nicalon SiC fiber was used in the following experiments.

In our investigations, tungsten and molybdenum were preferable materials for substrates compared to nickel. The primary reason is that their thermal expansion coefficients do not differ appreciably from that of silicon carbide ($\Delta\alpha$ = 1.5 x 10^{-6}/°k and 2.0 x 10^{-6}/°k for tungsten and molybdenum, respectively). When the tungsten substrate was used, the overcoating of the SiC fiber was successful except for minor peeling of the coating at the edges of the substrate. However, during the coating process, the tungsten became very brittle presumably due to H_2 in the gas mixture which is necessary to obtain a high quality silicon carbide coating. This embrittlement of substrate caused technical difficulty in ultimate testing of the sample; the sample shattered into brittle platelets when it was gripped in the microtensile test unit. When the molybdenum substrate was used, however, better adhesion of the SiC coating was obtained and somewhat less embrittlement of substrate was observed. Ion milled of the molybdenum substrate showed even better adhesion of the coating compared to unmilled substrate. Figure 6 shows a scanning electron micrograph of a cross section of the sample. A continuous coating from the substrate to the overcoating on the fiber is clear. However, there is a evidence of some reaction products between the silicon carbide and the molybdenum. Figures 7 and 8 compare scanning electron micrographs of the naked fiber and the silicon carbide coated fiber. The characteristic "corn cob" surface of chemically vapor deposited silicon carbide fiber is seen in Figure 8. Figure 9 shows the overcoated SiC fiber after four hours of coating time. It is seen that homogeneous layers adhere well to the fiber surface over the length and perimeter of the fiber. However, the fiber was not completely embedded in silicon carbide as shown in Figure 2. This problem was eliminated by increasing the coating time. Figure 10 shows the complete embedment of the fiber after 10 hours. Scanning electron

micrographs of the fractured cross section of this sample are shown in Figure 11. They clearly show the embedding of the SiC fiber by the grown silicon carbide layers. However, the adhesion of coating to the substrate was not as good as expected. This implies that there should be an optimum thickness of the CVD coating; the coating should be thick enough to achieve a complete embedment of fiber, yet be thin enough not to peel off the substrate.

The crystalline phases present in SiC deposited at 1050°C were identified by X-ray diffraction (Ni filtered Cu Kα). Representative X-ray diffraction patterns of the sample are shown in Figure 12. Only three distinguishable peaks were detected. The strongest lines corresponding to the (111) reflection of SiC was observed in the diffraction pattern. The sample consisted predominantly of the β-phase of SiC.There were no X-ray evidence for silicon which is usually observed in low temperature deposition[10].

IV CONCLUSIONS

A technique has been developed for fabricating single filament test specimens comprised of a SiC fiber embedded in SiC chemically vapor deposited on a molybdenum substrate. The CVD overcoating formed preferentially around the filament so that the specimen had the configuration shown in Figure 2. There appears to be good continuity between the coating around the fiber and the undercoating (Figure 11). This continuity is important for stress transfer from the metal substrate into the fiber.

The SiC layer was not well bonded to the molybdenum substrate due to the formation of a reaction layer between the two phases. The low bond strength prevented any meaningful mechanical testing of the specimen. This problem is not seen as insurmountable since a thin evaporated precoating of an inert metal (Pt, Au) on the molybdenum should prevent reaction with the SiC.

The specimen configuration developed here is not applicable to all possible fiber/matrix combinations. In the case of carbon fibers, there was evidence of the CVD reagent attacking the fiber (this observation has implications on the actual state of carbon fibers in a SiC matrix formed by vapor deposition of a chlorosilane). Furthermore, differences in the thermal coefficient of expansions of the fiber, matrix and substrate must be minimal. For the SiC/SiC/Mo system, the $\Delta\alpha$ was $2.0 \times 10^{-6}/°K$. Evidently, this difference is tolerable.

V RECOMMENDATIONS

The following recommendations are offered for continued work with SiC/SiC/Mo single filament specimen.

a) Find precoatings for the molybdenum substrate that prevent reaction with the SiC coating.
b) Mechanically test these specimens in tension to increasing strain levels.
c) Inspect the coated fiber for microcracks resulting from fiber breakage and brittle fracture of the SiC coating.
d) Use x-ray radiography to detect for fiber breaks and fiber/matrix debonding.
e) Expose the fiber (abrasion, alkaline etching , ion-milling) and inspect for fiber fracture and debonding.
f) Section through the specimen and examine (SEM, EDAX, and SAEM) for a fiber/matrix interlayer which may be a reaction layer or simply a difference in the matrix morphology.
g) Conduct the above experiments using coated fibers (BN, etc) and for SiC matrices formed from different CVD chemicals.

The embedded single fiber test for ceramic matrix system is seriously limited by the strong residual thermal stress that develops during specimen fabrication. At the very least, it limits the choice of materials that can be investigated to those having nearly equal thermal coefficients of expansion. Even in the case of the system reported here, SiC/SiC/Mo, thermal stresses may be comparable to the adhesion forces.

Alternative methods of investigating the interphase region in ceramic

matrix materials should be explored. The microindentation "push out" test is a likely candidate if the push-out force is measured as a function of specimen thickness so that the frictional adhesion can be readily distinguished from interphase fracture[11]. This approach is less ambiguous than simply measuring the indentation force and displacement[12].

VI. REFERENCES

1. E. Fitzerand R. Gadow, " Fiber Reinforced Silicon Carbide", Am. Ceram. Soc. Bull., 65, 326 (1986)

2. J. A. Cornie, Y. M. Chiang, D. R. Uhlman, A. Mortensen, and J. M. Collins, "Processing of Metal and Ceramic Matrix Composites", Am. Ceram. Soc. Bull., 65, 293 (1986)

3. E. C. Luh and A. G. Evans, "High Temperature Mechanical Properties of a Ceramic Composites", J. Am. Ceram. Soc., 70, 466 (1987)

4. R. A. Sambell, D. H. Bowen, and D.C. Phillips, "Carbon Fiber Composites with Ceramic and Glass Matrices, Part 1, Discontionuous Fibers", J. Mater. Sci., 7, 663 (1972)

5. R. A. Sambell, et. al.," Carbon Fiber Composites with Ceramic and Glass Matrices, Part 2, Continuous Fibers", ibid, 7, 676 (1972)

6. W. D. Bascom and R. M. Jensen, "Stress Transfer in Single Fiber/ Resin Tensile Tests", J. Adhesion, 19, 219 (1986)

7. W. Kern and V. S. Ban, "Chemical Vapor Deposition of Inorganic Thin Films " in Thin Film Processes edited by J. L. Vossen and W. Kern, Academic Press, 25 (1978)

8. K. K. Chawla, "Composite Materials-Science and Engineering", Spriger-Verlag, 37-57 (1987)

9. G. Verspui, "CVD of Silicon Carbide and Silicon Nitride on Tools for Electrochemical Machining" in Proc. of the Seventh International Conference on Chemical Vapor Deposition edited by T. O. Sedgwick et. al.", 463 (1979)

10. T. D. Gulden, " Deposition and Microstructure of Vapor-Deposited Silicon Carbide", J. Am. Ceram. Soc., 8, 424 (1968)

11. D. K. Shetty, "Shear-Lag Analysis of Fiber Push-Out Tests for Estimating Interfacial Friction Stress in Ceramic Matrix Composites", J. Am. Ceram. Soc. , 71, C107 (1988)

12. D. B. Marshall and W. C. Oliver, "Measurement of Interfacial Mechanical Properties in Fiber-Reinforced Ceramic Composites," J. Am. Ceram. Soc., 70, 542 (1987)

Table 1 Physical properties of metal substrates used in this experiment

	Ni*	W**	Mo**
Melting Point(°C)	1453	3387	2610
Linear Exp. Coef. (10^{-6}/°k) (at 20°C)	13.3	4.6	5.1
Crystal Structure	FCC	BCC	BCC

Source: * Good Fellow Metals Cambridge Ltd, Cambridge, England
,* Alpha Products, Danvers, Massachusetts

Table 2 Typical physical properties of carbon fiber

Density (gm/cm^3)	1.83
Diameter (μm)	6-7
Modulus (GPa)	230
Strength (GPa)	3.5
Linear Expansion Coefficient ($10^{-6}/°k$)	-0.1-0.5

+ Hercules Aerospace, Magna, Utah

Table 3 Typical physical properties of Nicalon SiC fiber

Density (gm/cm^3)	2.6
Diameter (μm)	10-20
Modulus (GPa)	180
Linear Exp. Coef. ($10^{-6}/°k$)	3.1
Strength at 20°C (GPa)	
As-Produced	2
After 1400°C (argon)	<1
Strength at 1400°C (oxygen)	<0.5
Creep Strain at 1300°C, 0.6GPa, 20h (%)	4.5

++ NASA-AMES Research Center, Moffet Field, California

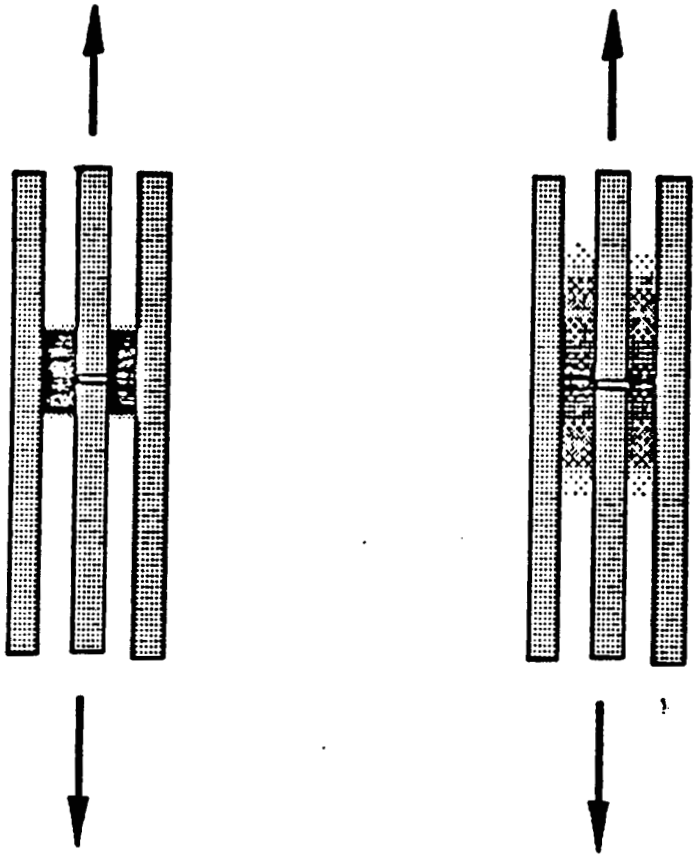

Figure1 Load sharing for strong bonding (A) and weak bonding (B)

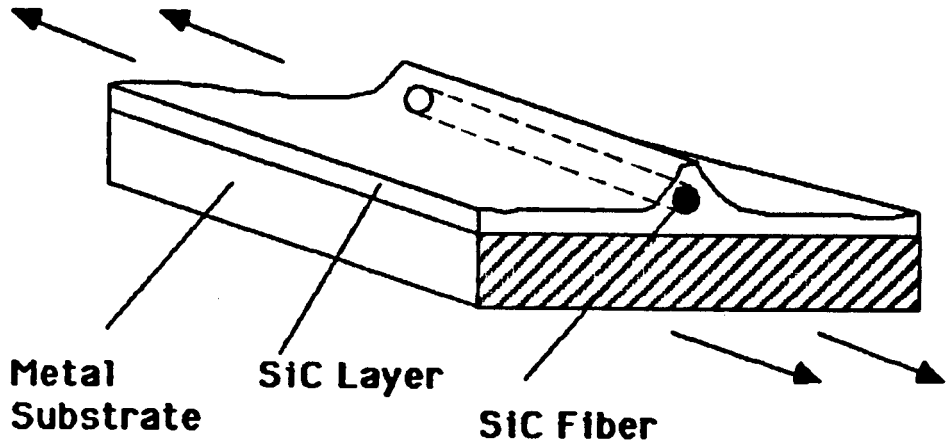

Figure 2 Schematic of a single filament in a coating of ceramic on a support plate

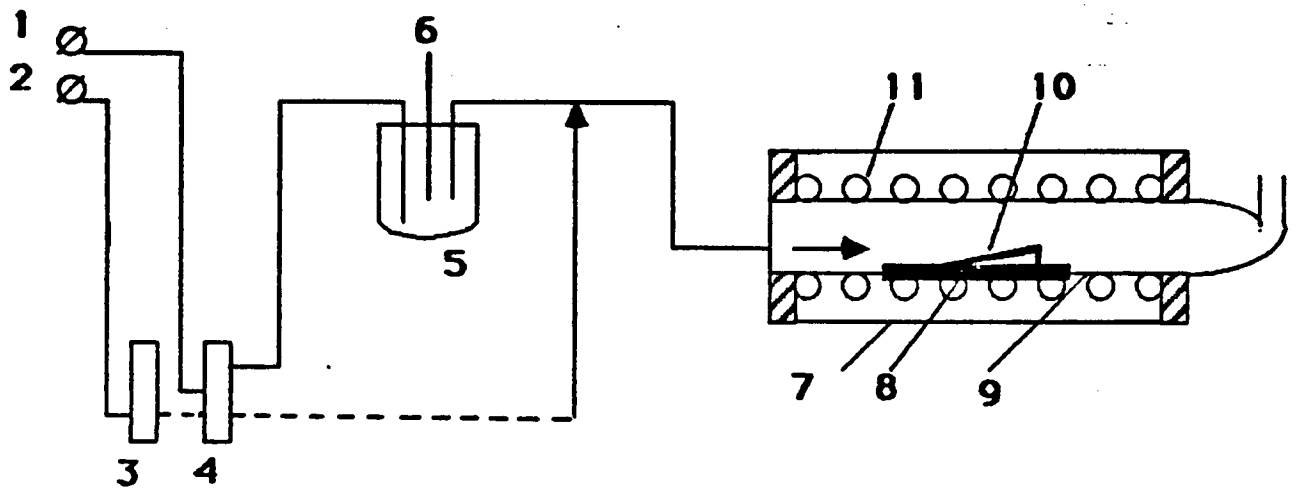

1. Argon Cylinder
2. Hydrogen Cylinder
3,4. Rotameter
5. Bubbler
6. Thermometer
7. Furnace
8. Silica boat
9. Silica tube
10. Metal Substrate
11. Heating Element

Figure 3 Schematic Diagram of Laboratory Reactor

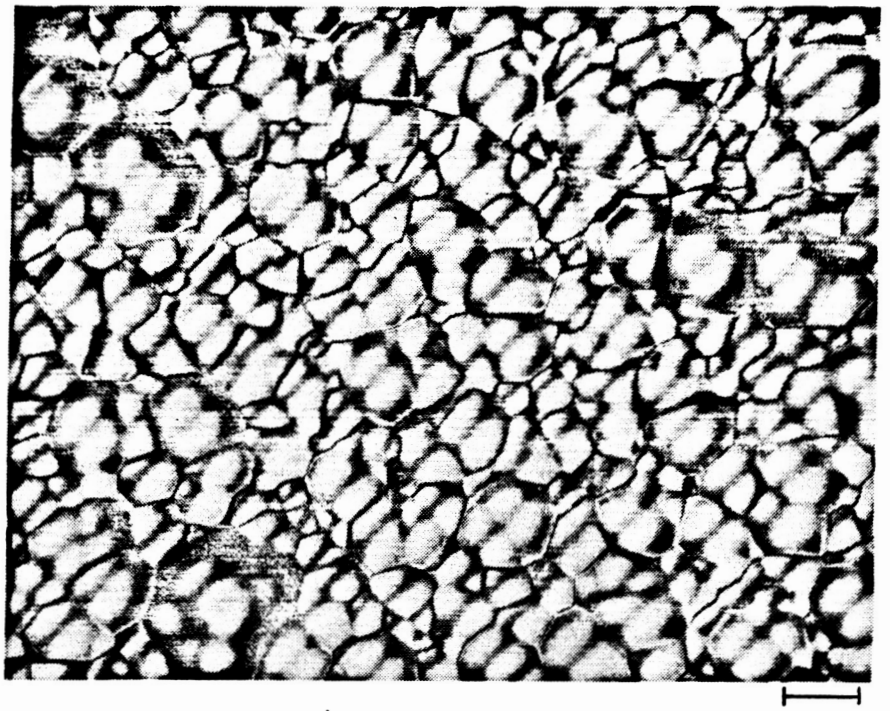

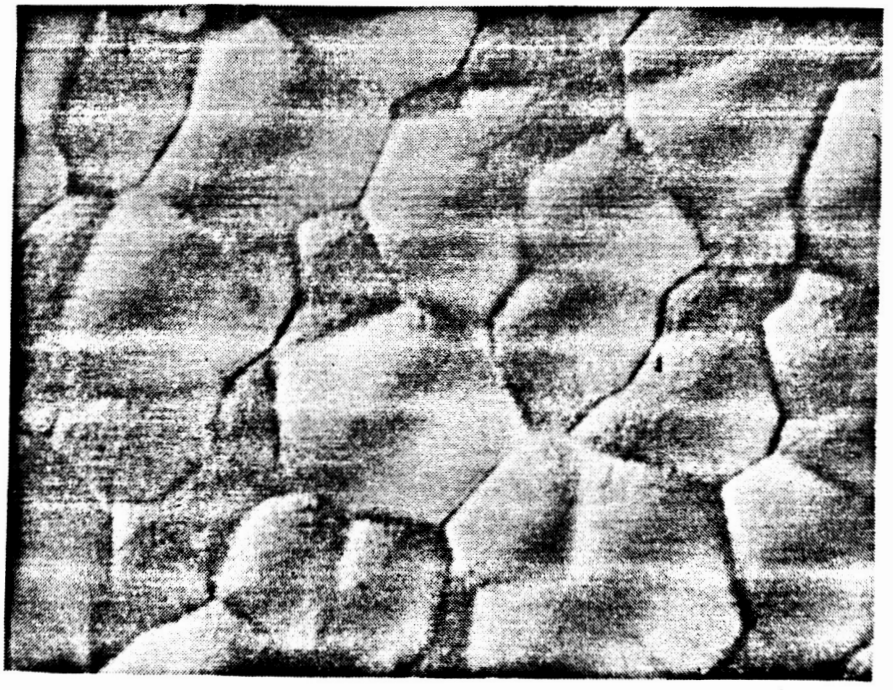

Figure 4 Optical micrographs of a silicon carbide undercoating on Nickel substrate

ORIGINAL PAGE IS
OE POOR QUALITY

Figure 5 Optical micrograph of cracks and peeling of the coating

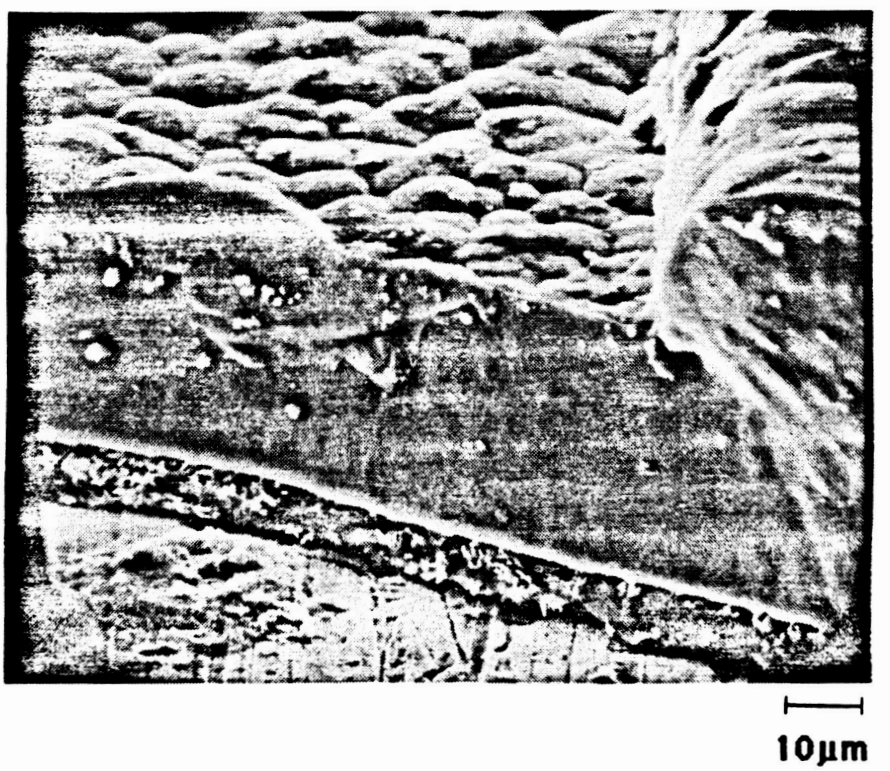

Figure 6 SEM photograph of a cross section of a sample

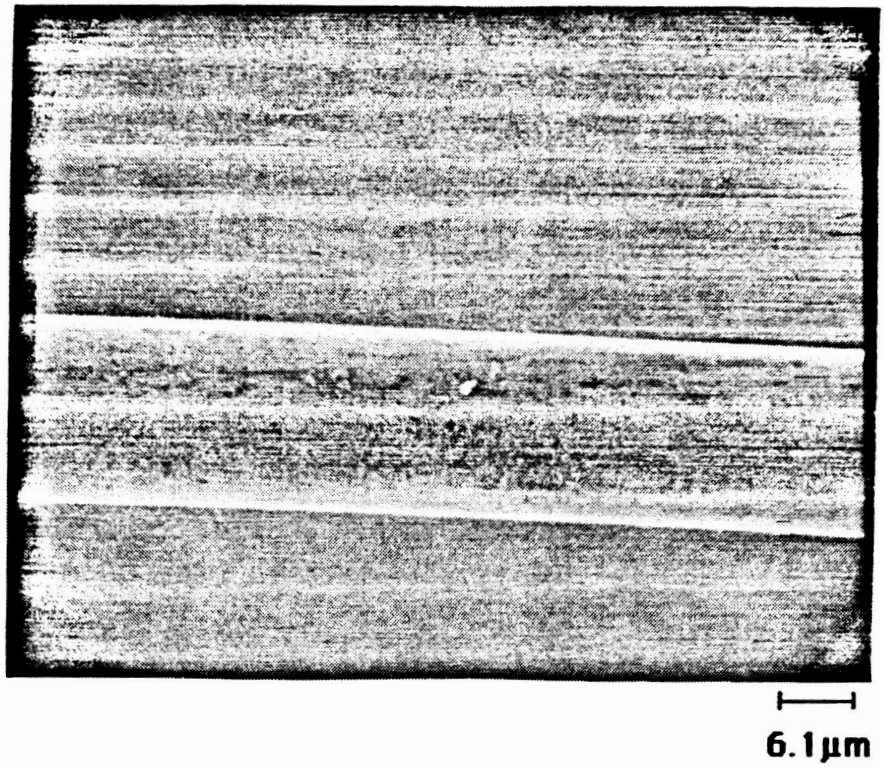

Figure 7 Uncoated Nicalon SiC Fiber

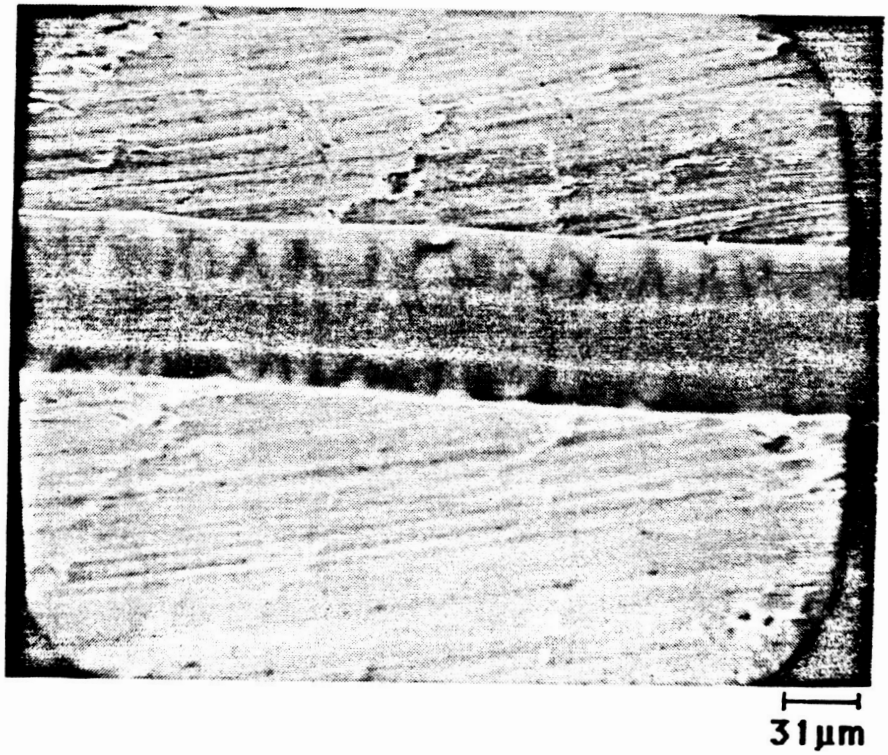

Figure 8 CVD coated Nicalon SiC fiber

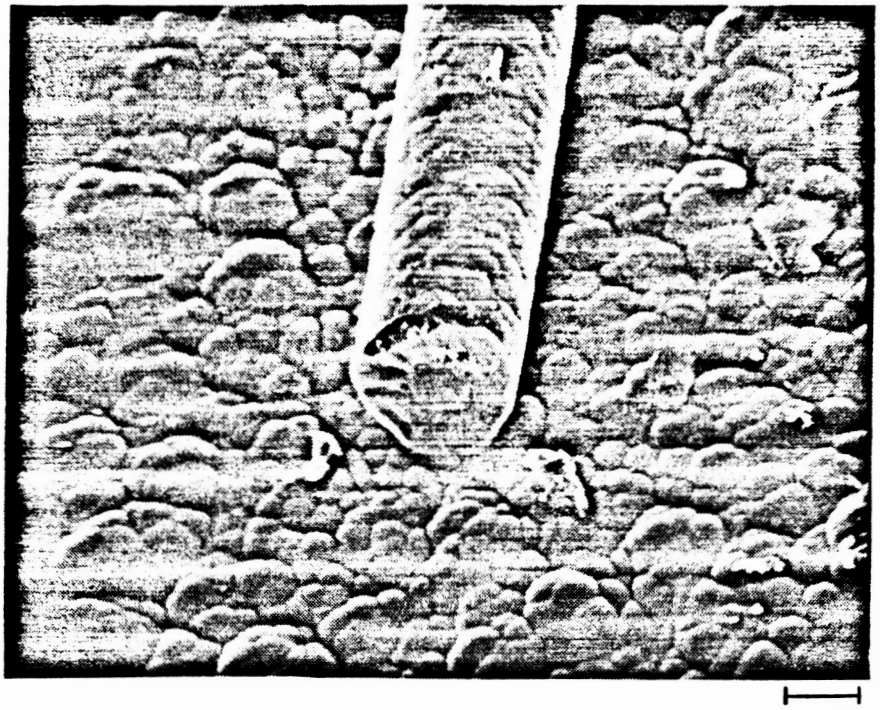

Figure 9 Overcoated SiC fiber after 4 hours coating time

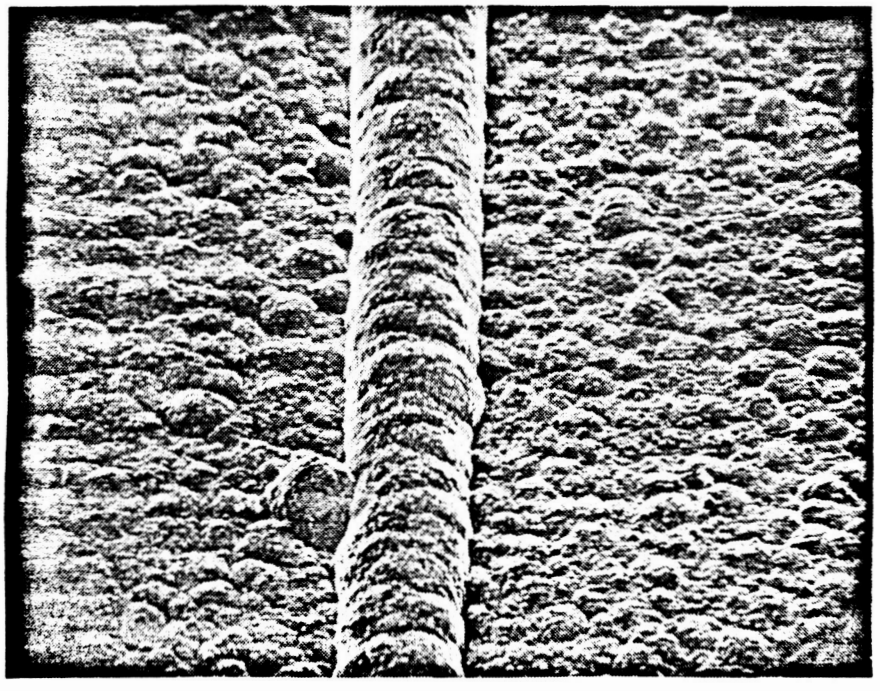

Figure 10 Overcoated SiC fiber after 10 hours coating time

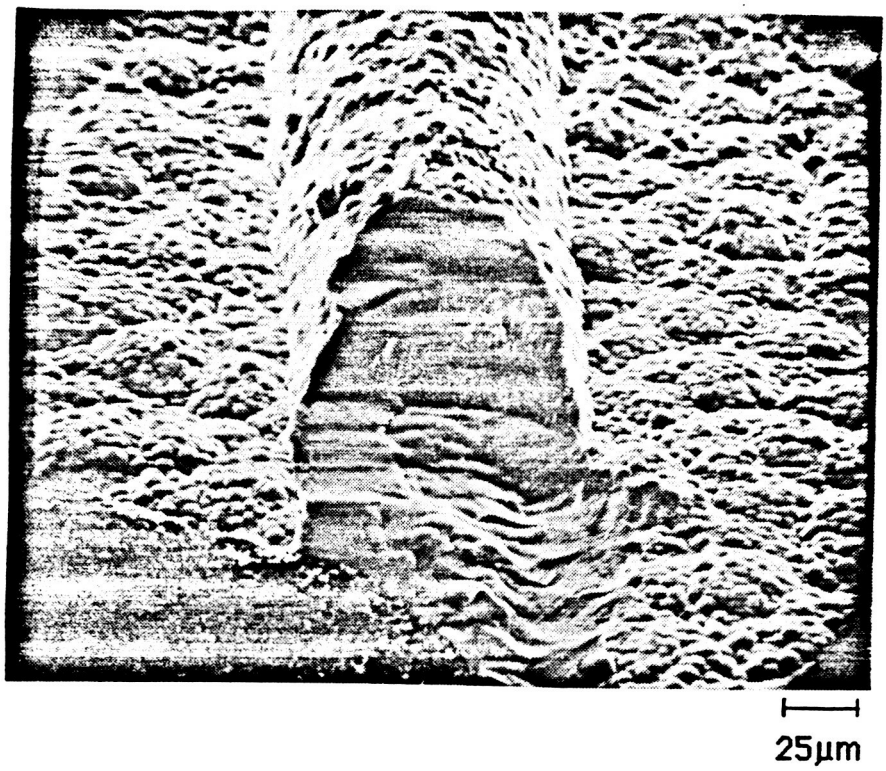

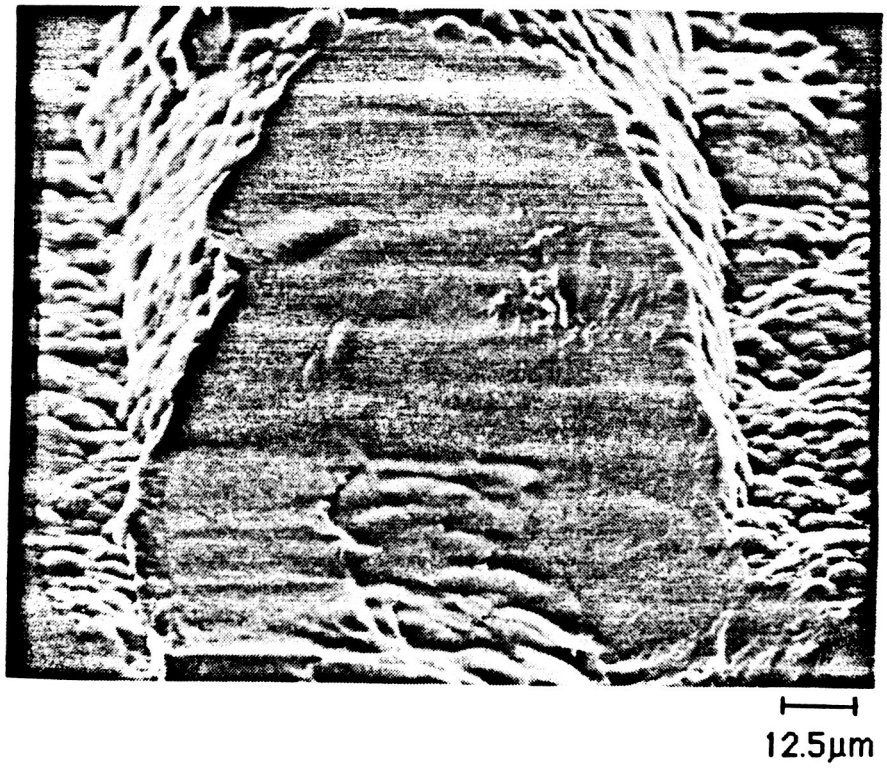

Figure 11 Scanning electron micrographs of fractured cross section

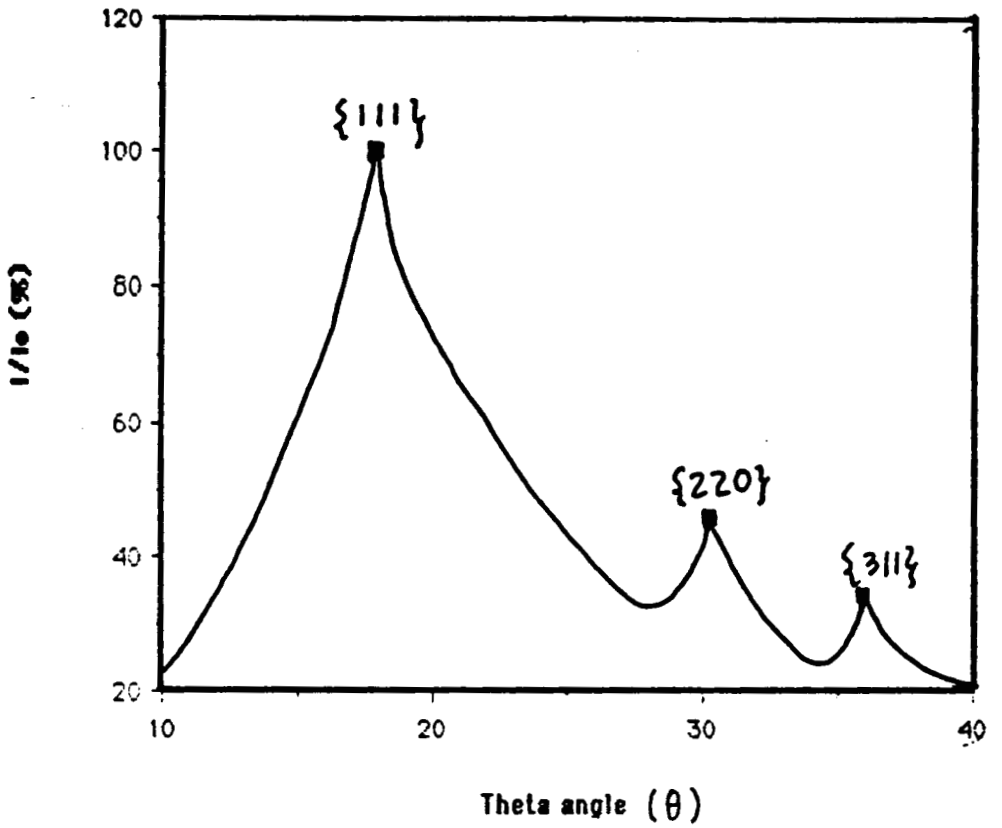

Figure 12 Profiles of X-ray diffraction pattern

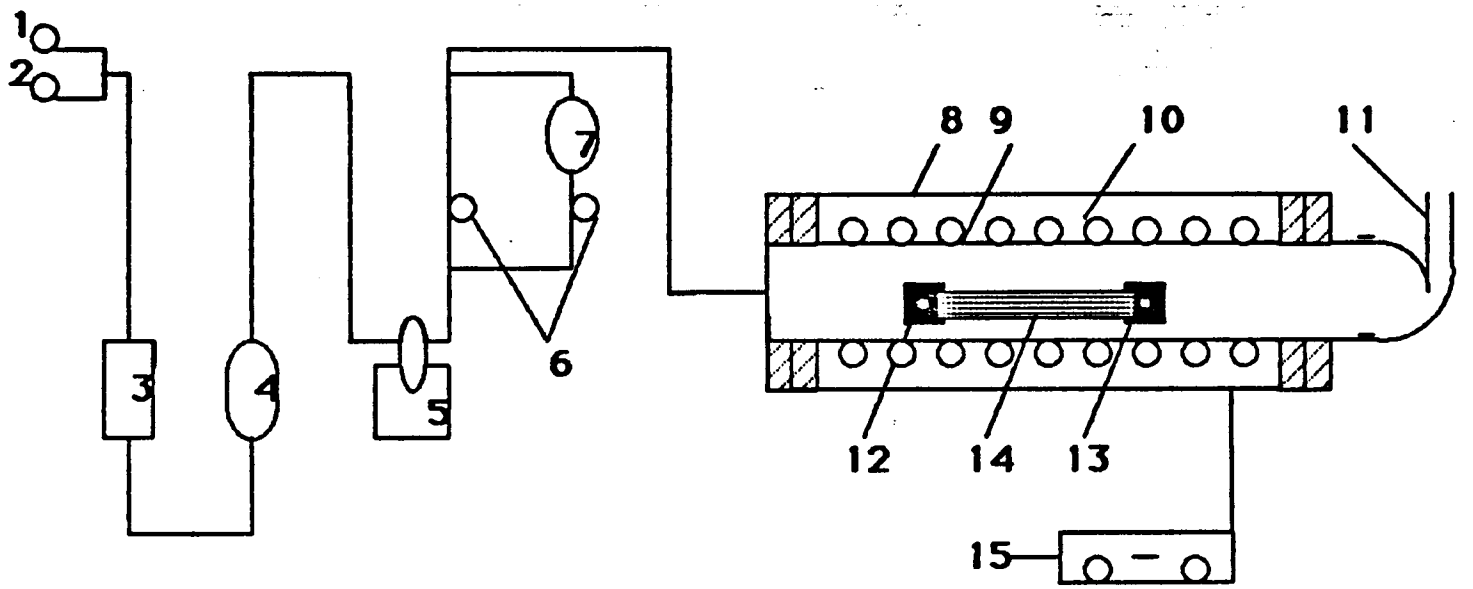

1. Hydrogen cylinder
2. Argon cylinder
3. Rotameter
4. 'Deoxo' catalyst
5. Cold trap
6. Metering valve
7. CH3SiCl3 container
8. Tube furnace
9. Quartz tube
10. Heating element
11. End cap
12-13. Graphite clamp
14. Substrate
15. Temperature programmer

Figure 13 CVD Apparatus for Deposition of SiC on to SiC Fiber